

# Design of an UHF Antenna Insensitive to the Concrete Dielectric Characteristics

Théo RICHARD<sup>a</sup>, Mohamed LATRACH<sup>a</sup>, Amine IHAMOUTEN<sup>b</sup>,  
Caroline BORDERON<sup>c</sup>, Hartmut W. GUNDEL<sup>c</sup> and Xavier  
DEROBERT<sup>d</sup>

<sup>a</sup>*ESEO-IETR, 10 Boulevard Jean Jeanneteau, 49100Angers*

<sup>b</sup>*Cerema, équipe ENDSUM Angers, 23 avenue de l'Amiral Chauvin, BP20069, 49136  
Les Ponts-de-Cé cedex*

<sup>c</sup>*IETR Nantes, UFR Sciences, 2 rue de la Houssinière, 44322 Nantes Cedex*

<sup>d</sup>*IFSTTAR, CS 04 - 44344 Bouguenaiscedex - France*

**Abstract.** In this communication, we present a design methodology for an insensitive radiating structure for concrete health monitoring applications. It takes advantage of an optimized smaller vacuum box surrounding a patch antenna. The Ansys HFSS software is used to simulate the studies of different configurations. The patch antenna consists of a radiating metallic element with a ground plane printed on a low-cost FR4 substrate. It is optimized to be linearly polarized and to be able to operate in free space medium at the first two resonant frequencies of 1.55 GHz and 1.95 GHz. This study demonstrates that a 5 mm high vacuum box above main radiating antenna, is sufficient to reduce the influence of three surrounding dielectric materials studied in this work, such as a PVC, concrete and limestone. Theoretical predictions, for all types of surrounded materials, show reasonably good agreement with experimental results.

**Keywords.** Insensitive antenna, concrete medium, nondestructive testing, UHF band.

## 1. Introduction

The main cause of deterioration of reinforced concrete in civil engineering structures is damage resulting from steel corrosion. Corrosion occurs when some aggressive agents, particularly chlorides in marine environments, penetrate through the protective cover concrete layer by means of various transfer mechanisms.

Nondestructive testing (NDT) techniques have become a useful tool for infrastructure experts in order to establish accurate diagnosis [1]. Electromagnetic NDT techniques are sensitive to the presence of water and chlorides in concrete, unlike mechanical NDT that are rather sensitive to porosity and to the mechanical properties of concrete structures [2].

From a durability point of view, periodical survey using electromagnetic NDT techniques is necessary. That makes structural health monitoring (SHM) with embedded devices allowing wireless transmission an extremely interesting tool.

The global objective of the present study is to develop an insensitive antenna that is able to work in presence of surrounding concrete medium. In fact, the electromagnetic properties of the concrete are difficult to quantify exactly and may

vary with frequency and moisture content. Consequently, we fixed two criteria to select the optimized antenna technology: the topology and the operating frequency.

A patch antenna was chosen due to its weak electric field in the near-coupling area [3-4]. Once the antenna selected, we performed various parametric studies in order to minimize the coupling effect between the antenna and the surrounding media. This leads to introducing and optimizing a smaller vacuum box around the proposed antenna.

## 2. Concrete characteristics and electromagnetic' properties

Before presenting parametric studies leading to the choice of the antenna structure, the global characteristics of concrete have to be recalled. Hydraulic concrete is an heterogeneous mixture of various materials: sand, aggregates, cement, water, ... It is well known [5] that the dielectric permittivity of the mixture depends on the nature of the cement, as well on the mineralogical nature of the aggregates and the water-to-cement ratio (W/C). Moreover, the permittivity of concrete mixtures evolves over time (due to hydration and aging phenomena) and is highly sensitive to the water, chloride and carbonation ingresses [6-9].

Fig .1 shows an experimental result [10] of the frequency dependence for the complex relative permittivity of concrete at different humidity conditions (0, 50, 75 and 100%). The characteristics of the studied mixture are calcareous aggregates, CEMI cement + AEA (air-entrained agent), cement ( $350 \text{ kg.m}^{-3}$ ) and W/C = 0.35. Although this mixture has a low porosity (low W/C), we can see a notable dependence of the complex relative permittivity on the water content. Furthermore, it is important to note that it remains almost constant for frequencies higher than 500 MHz.

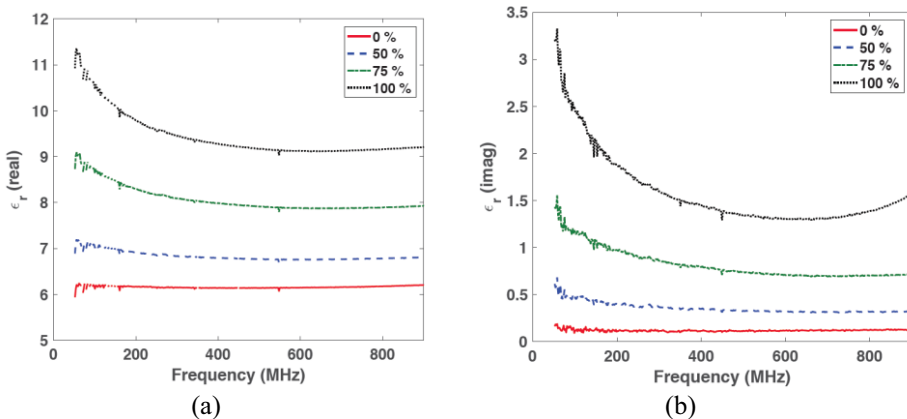


**Figure 1.** Real (a) and imaginary (b) parts of the permittivity of concrete versus frequency for four different humidity conditions.

As the globally dielectric properties of concrete depend on the mixture, on infrastructure aging, and on human/environmental impacts (uncontrolled phenomena), the main criterion for the antenna selection in our case should be its insensitivity to the varying dielectric properties of the surrounding medium.

### 3. Antenna structure

A patch antenna was chosen for its specific characteristics and, *inter alia*, a low electric in its near field zone [3]. It allows a very low coupling with the concrete surrounding medium and can meet the expectations of this study. Figure 2 shows the geometry of the used patch antenna. It consists of a metallic radiated element with ground plane printed on a low-cost FR4 substrate with relative permittivity  $\epsilon_r = 4.5$ . It was optimized by HFSS software [11] for efficient behavior in free space medium at the first two resonant frequencies around 1.55 GHz and 1.95 GHz. An example of the antenna positioning inside the reinforced concrete medium is shown in Fig. 3. This figure illustrates a smaller vacuum box surrounding the patch antenna. As the wireless transmission performance through a dielectric medium strongly depends on the coupling between the antenna and the material, we chose to minimize specifically the coupling conditions and their effects by optimizing the free space distance  $d$  between the antenna and the surrounding dielectric medium.

In the next sections, HFSS software simulations and experimental results will be compared, knowing that for both studies (numerical and experimental):

- the free space distance  $d$  varies from 0 to 50 mm in 1 mm steps.
- the relative permittivities of the transmission media were fixed to 2.7, 4.5, and 6.0, corresponding respectively to the permittivity values of PVC, limestone, and concrete.

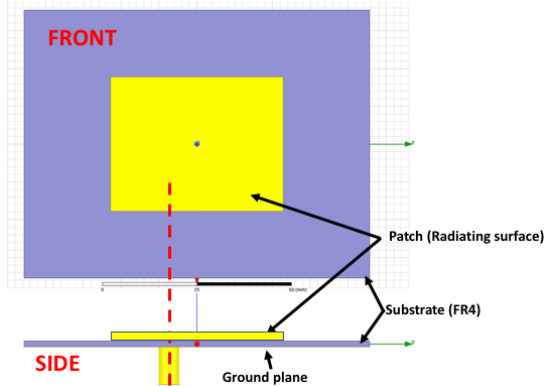


Figure 2. Optimized patch antenna layout: frontal view and side view.

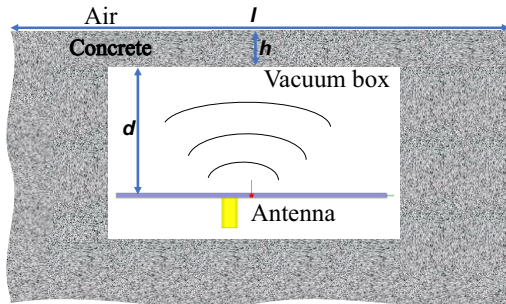


Figure 3. Geometry of study configuration

## 4. Results and discussion

### 4.1. HFSS simulation results

Fig. 4 shows HFSS numerical results corresponding to the evolution of the reflection coefficient ( $S_{11}$  parameter) of a patch antenna coupled to various modeled media (vacuum, PVC, limestone and concrete) at 3 positions ( $d = 0$  mm, 5 mm and 50 mm).

When the antenna is close to the transmission medium (Fig. 4a), it can be clearly seen as permittivity increases, resonant frequencies decrease and matching is degraded. At  $d = 5$  mm (Fig. 4b), a very small frequency shift can be observed, however there is still decrease the antenna matching between the vacuum case and the other media case and especially at the second resonant frequency (1.95 GHz). When the  $d$  distance between patch antenna and dielectric medium is further increased ( $d = 50$  mm, Fig. 4c), almost no frequency shift is visible anymore. At least in the case of the first resonance mode, the mismatch observed for the embedded antenna is almost similar to that of the antenna in vacuum. Therefore, it can be stated that the antenna is insensitive to the varying dielectric properties of the transmission/coupling medium.

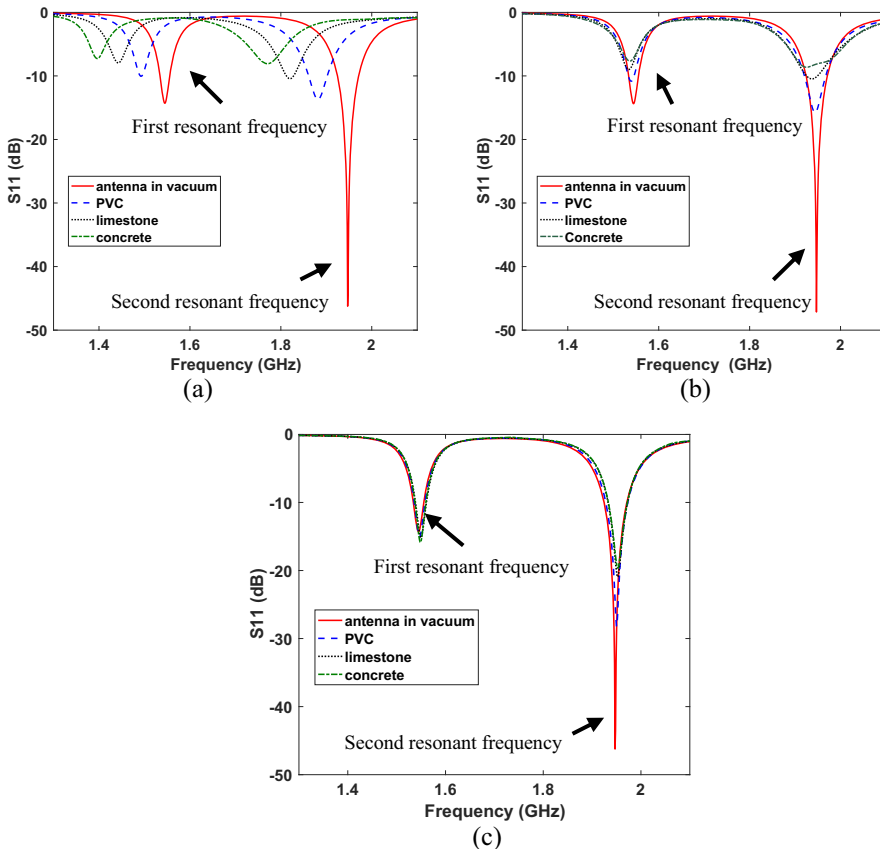


**Figure 4.** Simulated reflection coefficient  $S_{11}$  versus frequency for three distances  $d$  between the antenna and the three transmission medium studies.  $d = 0$  mm (a),  $d = 5$  mm (b),  $d = 50$  mm (c).

Fig. 5 illustrates the evolution of the two first resonant frequencies as a function of the distance between the antenna and the considered transmission medium. The horizontal solid line (red line) corresponds to the vacuum resonance frequency, which can be considered as a reference.

For the first resonance modes, we can observe that both resonant frequencies are constant for all media at a distance  $d$  around 5 mm. At that specific distance, the resonant frequency is very close to that observed for the vacuum case. Except for large distances ( $d > 50$  mm), where obtained vacuum resonant frequency is get closer and closer to one another. The distance  $d = 5$  mm seems to be adapted for EM wave transmission with very low dependence on the varying dielectric properties of the transmission/coupling medium.

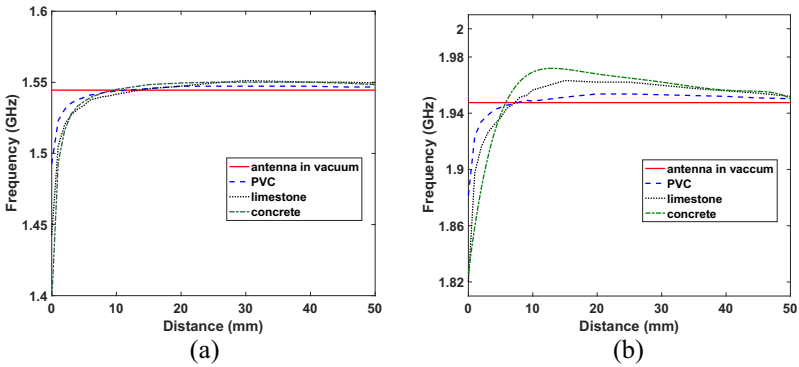


**Figure 5.** Antenna resonance frequencies versus distance between the antenna and the considered transmission media ( $\epsilon_{r,PVC} = 2.7$ ,  $\epsilon_{r,limestone} = 4.5$ ,  $\epsilon_{r,Concrete} = 6.0$ ). First (a) and second (b) resonant frequency.

#### 4.2. Experimental results

The patch antenna characteristics (in free space and coupled to PVC, limestone and concrete slabs) were experimentally determined. The dielectric characteristics of selected materials were measured using a coaxial transmission line. The PVC, concrete, and limestone slab dimensions were respectively  $1\text{ m} \times 1\text{ m} \times 0.2\text{ m}$ ,  $1\text{ m} \times 1\text{ m} \times 0.12\text{ m}$ , and  $0.5\text{ m} \times 0.5\text{ m} \times 0.2\text{ m}$ .

The  $S_{11}$  measurements were done per millimeter up to  $d = 50$  mm using an automatic experimental platform and a vector network analyzer (VNA).

The experimental evolution of the reflection coefficient ( $S_{11}$  parameter) of the patch antenna coupled to the studied media (vacuum, PVC, limestone and concrete) at three positions ( $d = 0$  mm, 5 mm and 50 mm) is shown in Fig. 6.

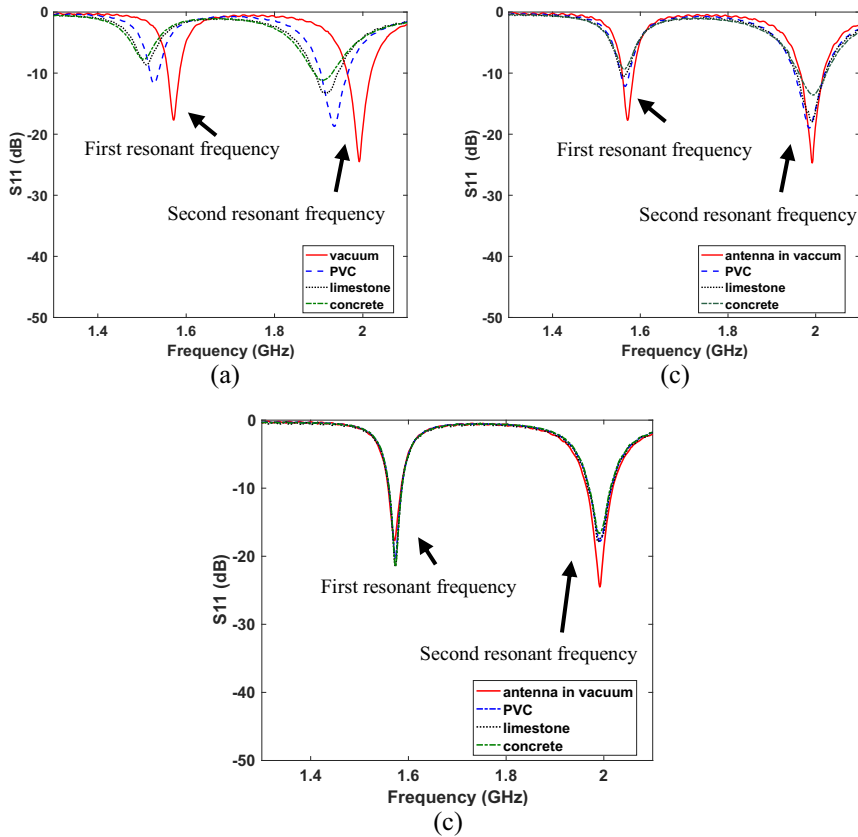


**Figure 6.** Measured reflection coefficient  $S_{11}$  versus frequency for three distances  $d$  between the antenna and the transmission medium as PVC, limestone, and concrete.  $d = 0$  mm (a),  $d = 5$  mm (b),  $d = 50$  mm (c)

The experimental results are very similar to those of the numerical study even though the relative frequency shifts are smaller for limestone and concrete (Fig. 6a). Limestone is rather sensitive to the ambient humidity that cannot be controlled, thus probably causing modified dielectric properties compared to the initial characterization. The fabricated concrete slab is not homogenous unlike what was defined in the HFSS simulation.

At  $d = 5$  mm (Fig. 6b), only a small frequency shift can be observed, however, there is still an increase in impedance mismatch for the three used media. When the antenna/medium distance is further increased ( $d = 50$  mm, Fig. 6c), almost no frequency shift is visible anymore, which is in accordance with the numerical results. We can conclude that above  $d = 5$  mm, the studied patch antenna is insensitive to the varying dielectric properties of the environmental medium.

The evolution of the resonant frequencies as a function of the distance between the antenna and the transmission medium for the three modeled media is illustrated in Fig. 7. Again, the horizontal solid line (red line) corresponds to the vacuum resonance frequency.

For the first resonance modes, we can observe a both resonant frequencies are constant for all media at a distance  $d$  around 5 mm. At this specific distance, the

resonance frequency is very close to that observed in the vacuum case. In agreement with the simulation results, the 5 mm high vacuum box seems to be adapted for the proposed antenna without any dependence on the varying dielectric properties of the surrounding medium.

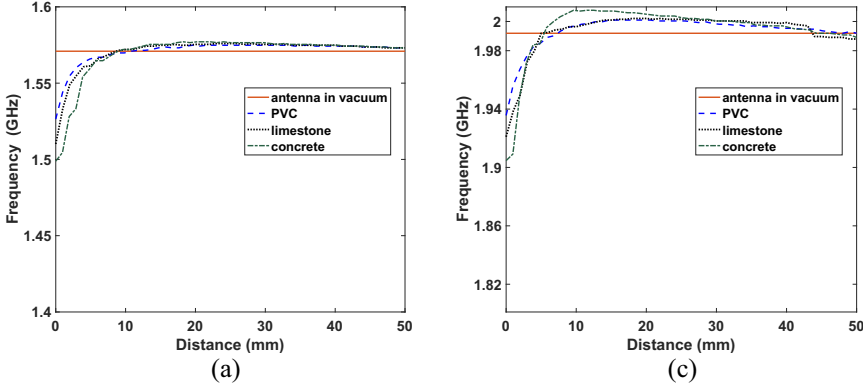


**Figure 7.** Measured antenna resonance frequencies *versus* distance between the antenna and the surrounding media. First (a) and second (b) resonance frequency.

Table 1 provides numerical and experimental results for the case study where  $d = 5$  mm (Figs. 4b and 6b). This highlights the very good correspondence between simulations and experiments results. We can especially note that the chosen patch antenna is insensitive to the varying dielectric properties of the surrounding medium for a 5 mm high air gap of in above the antenna.

**Table 1.**  $S_{11}$  magnitude, resonant frequencies, and frequency shift  $\Delta f$  with respect to free space transmission for the different antenna surrounding media. Exp = experiment, Sim = simulation.

	FIRST RESONANCE FREQUENCY						SECOND RESONANCE FREQUENCY					
	$S_{11}$ (dB)		$f_1$ (GHz)		$\Delta f$ (%) = $\frac{f_1 \text{ vacuum} - f_1 \text{ medium}}{f_1 \text{ vacuum}}$		$S_{11}$ (dB)		$f_2$ (GHz)		$\Delta f$ (%) = $\frac{f_2 \text{ vacuum} - f_2 \text{ medium}}{f_2 \text{ vacuum}}$	
	Sim	Exp	Sim	Exp	Sim	Exp	Sim	Exp	Sim	Exp	Sim	Exp
<b>Vacuum</b>	-14.37	-17.72	1.54	1.57	-	-	-47.14	-24.72	1.95	1.99	-	-
<b>PVC</b>	-10.83	-12.17	1.54	1.56	0.3%	0.4%	-15.76	-19.03	1.94	1.99	0.2%	0.4%
<b>Limestone</b>	-8.99	-10.58	1.53	1.56	0.7%	0.4%	-10.47	-17.97	1.94	1.99	0.5%	0,0%
<b>Concrete</b>	-7.66	-9.35	1.53	1.56	0.5%	0.4%	-7.66	-13.58	1.93	1.99	1.1%	0,0%

### 5. Conclusions

The main goal of the present study was to obtain an insensitive antenna configuration to allow precise transmission across a concrete structure. This includes only little dependency on the dielectric properties of its surrounding medium, which vary with

humidity, aging and several environmental conditions like pathogen agents. The performed simulation and experiments confirm that a 5 mm high vacuum box above main radiating antenna, allows the antenna to be insensitive to the surrounding dielectric characteristics. This is due to the intrinsic characteristic of a patch antenna, which radiate a weak electric in its near-field zone.

Under the investigated conditions, a frequency shift of less than 1% around the first two resonant frequencies (1.55 GHz and 1.99 GHz) first of the antenna has been obtained, proving the insensibility of the antenna to the surrounding medium.

This study was focused on the analyses of the reflection coefficient of the antenna surrounded by homogenous dielectric medium. In the future, the radiating characteristics of the embedded antenna, taking in to account medium losses, will be studied.

## 6. Acknowledgements

The present work has been performed in the frame work of the DADIM-PdL research project supported by the French Pays de la Loire region. The financial support is gratefully acknowledged.

## References

- [1] D. M. McCann and M. C. Forde, Review of NDT methods in the assessment of concrete and masonry structures, *NDT&E Int* (2001), 71–84.
- [2] J. P. Balayssac, S. Laurens, G. Arliguie, D. Breyse, V. Garnier, X. Dérobert and B. Piwakowski, Description of the general outlines of SENSO project: Quality assessment and limits of different NDT methods, *Journ. Const. & Build. Mat.* **35** (2012), 131-138.
- [3] C. A. Balanis, *Antenna theory: analysis and design*, John Wiley & Sons, 2016.
- [4] X. Jin and M. Ali, Embedded antennas in dry and saturated concrete for application in wireless sensors, *Progress in electromagnetics research* **102** (2010), 197–211.
- [5] X. Dérobert and G. Villain, Development of a multi-linear quadratic experimental design for the EM characterization of concretes in the radar frequency-band, *Constr Build Mat* (2016), 237-245.
- [6] A. Robert, Dielectric permittivity of concrete between 50 MHz and 1 GHz and GPR measurements for building materials evaluation, *J Appl Geophys* (1998), 89-94.
- [7] K. J. Bois, A. D. Benally, P. S. Nowak and R. Zoughi, Cure-state monitoring and water-to-cement ratio determination of fresh Portland cement-based materials using near-field microwave techniques, *IEEE Trans Instrum Meas* (1998), 628-37.
- [8] M. N. Soutsos, J. H. Bungey, S. G. Millard, M. R. Shaw and A. Patterson, Dielectric properties of concrete and their influence on radar testing, *NDT & E Int* (2001), 419–25.
- [9] X Dérobert and G. Villain, EM characterization of concretes focused on water and chloride contents in the frame of multi-linear experimental designs, *GPR2016 Proceedings* (2016).
- [10] IFSTTAR, *internal report*, Bouguenais – France, 2017.
- [11] ANSYS, *HFSS v18.2*, [www.ansys.com](http://www.ansys.com), 2017